PNAS RESEARCH ARTICLE | BIOCHEMISTRY

Germline *C1GALT1C1* mutation causes a multisystem chaperonopathy

Florian Erger[a,b,1], Rajindra P. Aryal[c,1], Björn Reusch[a,b], Yasuyuki Matsumoto[c], Robert Meyer[d], Junwei Zeng[c,e], Cordula Knopp[d], Maxence Noel[c], Lukas Muerner[c,f], Andrea Wenzel[a,b], Stefan Kohl[g], Nikolai Tschernoster[a,b,h], Gunter Rappl[b], Isabelle Rouvet[i], Jutta Schröder-Braunstein[j], Felix S. Seibert[k], Holger Thiele[h], Martin G. Häusler[l], Lutz T. Weber[g], Maike Büttner-Herold[m], Miriam Elbracht[d], Sandra F. Cummings[c], Janine Altmüller[b,h,n,o], Sandra Habbig[g], Richard D. Cummings[c,2], and Bodo B. Beck[a,b,2]

Edited by Hudson H. Freeze, Sanford Burnham Prebys Medical Discovery Institute, La Jolla, CA; received June 28, 2022; accepted March 28, 2023 by Editorial Board Member Jasper Rine

Mutations in genes encoding molecular chaperones can lead to chaperonopathies, but none have so far been identified causing congenital disorders of glycosylation. Here we identified two maternal half-brothers with a novel chaperonopathy, causing impaired protein O-glycosylation. The patients have a decreased activity of T-synthase (*C1GALT1*), an enzyme that exclusively synthesizes the T-antigen, a ubiquitous O-glycan core structure and precursor for all extended O-glycans. The T-synthase function is dependent on its specific molecular chaperone Cosmc, which is encoded by X-chromosomal *C1GALT1C1*. Both patients carry the hemizygous variant c.59C>A (p.Ala20Asp; A20D-Cosmc) in *C1GALT1C1*. They exhibit developmental delay, immunodeficiency, short stature, thrombocytopenia, and acute kidney injury (AKI) resembling atypical hemolytic uremic syndrome. Their heterozygous mother and maternal grandmother show an attenuated phenotype with skewed X-inactivation in blood. AKI in the male patients proved fully responsive to treatment with the complement inhibitor Eculizumab. This germline variant occurs within the transmembrane domain of Cosmc, resulting in dramatically reduced expression of the Cosmc protein. Although A20D-Cosmc is functional, its decreased expression, though in a cell or tissue-specific manner, causes a large reduction of T-synthase protein and activity, which accordingly leads to expression of varied amounts of pathological Tn-antigen (GalNAcα1-O-Ser/Thr/Tyr) on multiple glycoproteins. Transient transfection of patient lymphoblastoid cells with wild-type *C1GALT1C1* partially rescued the T-synthase and glycosylation defect. Interestingly, all four affected individuals have high levels of galactose-deficient IgA1 in sera. These results demonstrate that the A20D-Cosmc mutation defines a novel O-glycan chaperonopathy and causes the altered O-glycosylation status in these patients.

Cosmc | *COSMC*-CDG | *C1GALT1C1* | O-glycosylation | Tn-antigen

Significance

We identify a novel chaperonopathy causing altered protein O-glycosylation. We describe the first cases of this multisystem disorder caused by a germline loss-of-function variant in *C1GALT1C1*. *C1GALT1C1* encodes Cosmc, an exclusive chaperone of the T-synthase, the enzyme that initiates complex O-glycan biosynthesis. As complex O-glycans are required for many cellular functions, the decrease in T-synthase activity caused by loss of Cosmc leads to a loss of mature O-glycans and a severe but partially treatable clinical phenotype. This discovery will promote a better understanding of the role of complex O-glycans in human health and disease.

Functional impairment of molecular chaperones can lead to multiple human disorders termed chaperonopathies (1). However, defects in molecular chaperones that regulate protein glycosylation are not well described. Glycosylation is one of the most common post-translational modifications of proteins, and is required for diverse cellular functions including cell–cell interactions, immune response, cell growth, and tissue formation (2–6). Glycan structures are assembled by the concerted action of a large number of enzymes and other proteins. Loss-of-function variants in genes encoding such proteins can lead to congenital disorders of glycosylation (CDG), which are mostly severe, syndromic diseases often presenting in infancy (7).

A common modification of glycoproteins is the addition of O-glycans linked via N-acetylgalactosamine (GalNAc) to serine, threonine and tyrosine residues through a multi-step process in the secretory pathway. The initiation of such elaborate O-glycans, which are based on the core 1 O-glycan structure (also called T-antigen; Galβ3GalNAcα1-O-Ser/Thr/Tyr; Fig. 1*A*), requires the action of a single Golgi enzyme T-synthase (encoded by *C1GALT1*) (8). However, folding and activity of the T-synthase are uniquely regulated by a single, specific endoplasmic reticulum-localized molecular chaperone called Cosmc, encoded by X-chromosomal *C1GALT1C1 (COSMC)* (8–10).

Complete germline knockout of either *C1galt1* or *C1galt1c1* in mice results in embryonic lethality (9, 13) and system-wide accumulation of T-antigen's immature precursor glycan, the Tn-antigen (GalNAcα1-O-Ser/Thr/Tyr; CD175). Partial loss-of-function models exhibit thrombocytopenia, bleeding diathesis, and smaller body size (1). Mice with a partial *C1galt1* knock-out developed severe proteinuric kidney disease with glomerular loss in renal histology (14), as do mice with podocyte-specific knockout of

Preprint Server: https://doi.org/10.21203/rs.3.rs-1716400/v1 (CC BY 4.0 License).

The authors declare no competing interest.

This article is a PNAS Direct Submission. H.H.F. is a guest editor invited by the Editorial Board.

[1]F.E. and R.P.A. contributed equally to this work.

[2]To whom correspondence may be addressed. Email: rcummin1@bidmc.harvard.edu or bodo.beck@uk-koeln.de.

This article contains supporting information online at https://www.pnas.org/lookup/suppl/doi:10.1073/pnas.2211087120/-/DCSupplemental.

Published May 22, 2023.

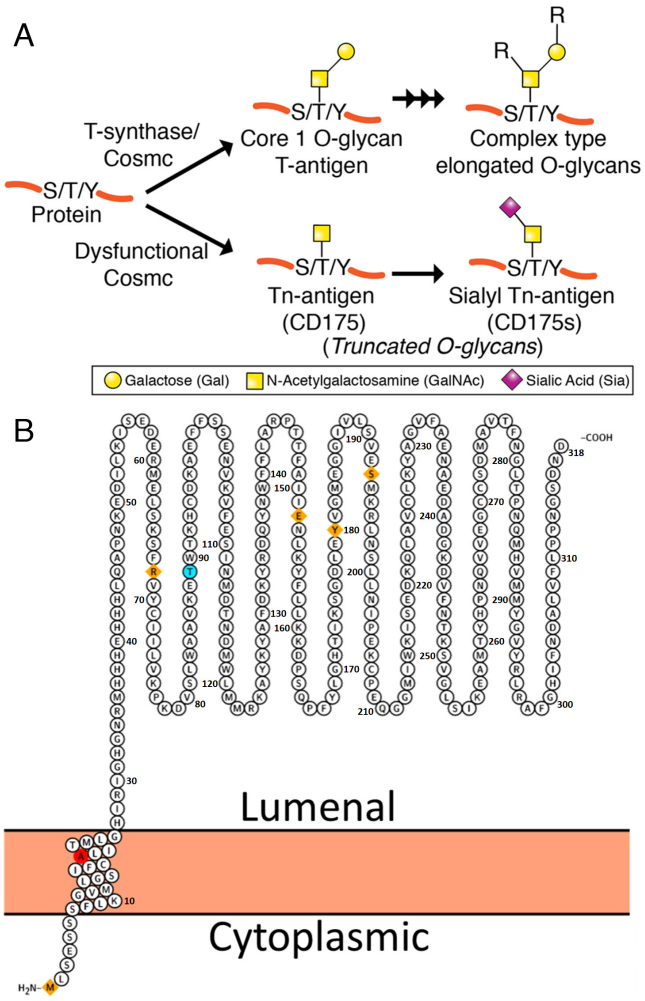

Fig. 1. (*A*) Schematic of O-glycan biosynthesis. Cosmc is an ER-localized molecular chaperone required for T-synthase function. T-synthase is critical for the generation of normal elongated O-glycans at serine, threonine, and tyrosine (S/T/Y) residues in glycoproteins. In the absence of functional Cosmc, T-synthase remains inactive and is degraded, resulting in truncated O-glycans. (*B*) Visualization of the transmembrane topology of full-length Cosmc protein. The red-filled alanine residue is mutated in patients M1, M2, F1, and F2. The orange-filled residues were affected by somatic mutations in previously reported patients with Tn syndrome. The light blue residue was affected in a recent single case publication of a patient carrying a de novo variant (c.266C>T; p.Thr89Ile) in *C1GALT1C1* (11). Protein visualization modified from Protter output (12).

C1galt1c1 (15). Altered expression of *C1GALT1* and/or *C1GALT1C1* is linked to IgA nephropathy (IgAN) in humans, in which Tn-antigen is enriched among the O-glycans of IgA1, which is termed galactose-deficient IgA1 (Gd-IgA1) (16–18). In IgAN, the autoantigenic Gd-IgA1 forms macromolecular circulating immune complexes (CICs), some of which are deposited into the glomerular mesangium over time, where they promote an inflammatory response (19–21).

In humans, somatic loss-of-function variants in *C1GALT1C1* affecting cells in the hematopoietic system can cause Tn syndrome, a rare and usually subclinical disorder presenting with mild hemolytic anemia, thrombocytopenia and leukopenia associated with Tn-antigen accumulation on a subset of blood cells (22, 23). Exposure of the abnormal Tn-antigen likely leads to an autoantibody-mediated cytotoxic immune response (24).

Here we report a family with two severely affected male and two mildly affected female patients carrying a germline missense variant in the X-chromosomal *C1GALT1C1* gene. This variant leads to a significant loss of Cosmc chaperone expression and subsequently causes a substantial reduction in T-synthase activity in hemizygous males with diverse O-glycan phenotypes. The patients' complex clinical and biochemical phenotypes arising from the tissue-variable disruption of normal O-glycosylation is termed *COSMC*-CDG. The clinical and functional investigations in these patients have substantially advanced our understanding of glycobiology and raise—from bedside to bench—intriguing questions about the role of the complement system in disorders of glycosylation.

Results

Clinical Presentation. We identified two male patients M1 and M2, half-brothers born of non-consanguineous German parents. Patient M1 is a 7-y–old child whose postnatal clinical course was marked by congenital pneumonia with persistent pulmonary hypertension requiring high-frequency oscillation ventilation. During infancy, he presented with recurrent infections, as well as chronic mild to moderate thrombocytopenia, chronic severe lymphopenia (repeatedly <300 /μL) and hypogammaglobulinemia (<300 mg/dL). Subaortic stenosis leading to myocardial hypertrophy was treated surgically at the age of 4 y, but has since recurred. The patient has disproportionate short stature with short arms and legs, as well as a high forehead, retrognathia, and downturned corners of the mouth (Fig. 2 *B* and *C*). The boy has global developmental delay with an intelligence quotient equivalent of <55 points at the age of 6 years, which is in the range of moderate intellectual disability. Patient M1 additionally developed generalized seizures in the neonatal period that were well-controlled pharmacologically. He attends a school for children with learning disabilities.

At the age of 5 y and 2 mo, the patient M1 was admitted to the pediatric intensive care unit with acute kidney injury (AKI) stage 3 requiring peritoneal dialysis for 20 d. The AKI was accompanied by gross proteinuria [serum albumin 24 g/L (Ref. 35 to 52 g/L)] with severe edema. Laboratory testing showed the typical signs of thrombotic microangiopathy (TMA) with Coombs-negative hemolytic anemia, thrombocytopenia, increased lactate dehydrogenase and schistocytosis in the peripheral blood smear. While shiga toxin polymerase chain reaction (PCR) was negative and ADAMTS13-activity proved normal, complement analysis showed dysregulation of the alternative complement pathway with reduced complement factor 3 and increased sC5b-9 in line with renal TMA or atypical hemolytic uremic syndrome (aHUS; *SI Appendix*, Table S1). Treatment with C5-inhibition (Eculizumab) resulted in the recovery of renal function within 10 d and proteinuria improved to <1 g/g creatinine per day within 6 wk. After negative genetic testing for all known aHUS-associated genes and given the very stable clinical course, Eculizumab treatment was discontinued 12 mo after initial presentation. Concomitant with laboratory evidence of loss of effective C5-inhibition, proteinuric AKI recurred but again showed complete response to re-initiation of C5-inhibition (Fig. 3).

Patient M2 is the 21-y–old maternal half-brother of patient M1. Within the first three months of life, he had severe thrombocytopenia (16,000/μL) accompanied by anemia (7.4 g/L), leukopenia (4,600/μL) and moderate neutropenia (550/μL). A bone marrow biopsy at 7 wk showed no pathological changes. Throughout childhood, the patient was repeatedly hospitalized with pneumonia, middle ear infections and gastrointestinal infections, although the frequency and severity of these infections decreased in adolescence. The patient had global developmental delay and went to a school for children with learning disabilities.

After clinical diagnosis of a syndromic nephropathy in his half-brother, we also evaluated patient M2 at the age of 20 y, who presented in good clinical condition with only minor

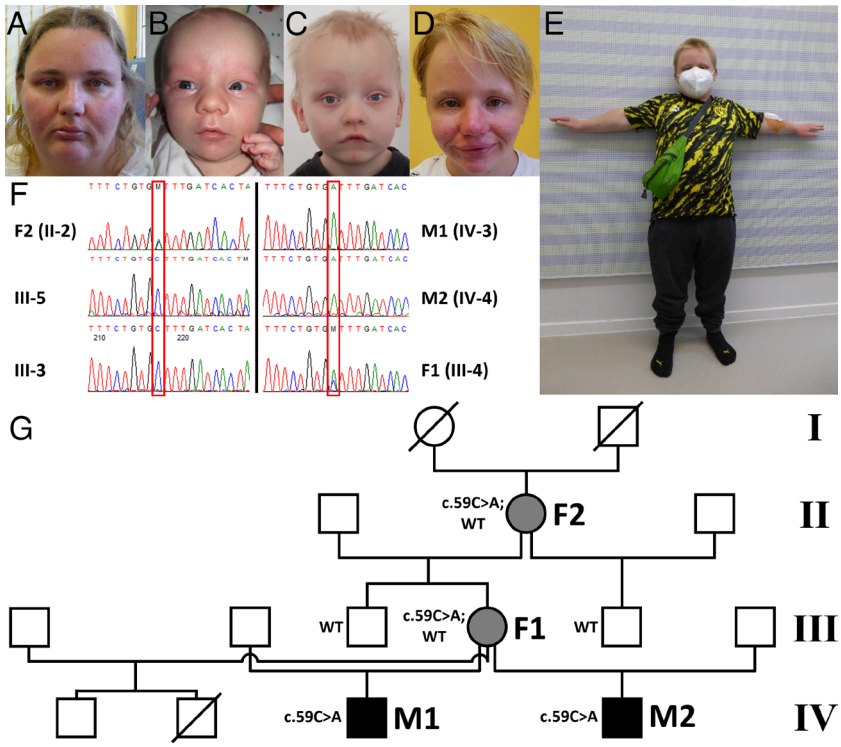

Fig. 2. Pedigree and photographs of reported patients. (*A*) Frontal facial photograph of patient F1 at the age of 38. (*B* and *C*) Frontal facial photograph of patient M1 at the age of 15 d and 4 y, respectively. (*D* and *E*) Frontal facial and whole-body photographs of patient M2 at the age of 20. Shared facial features are retrognathia, prominent nasolabial folds and a tall forehead, patient M2 shows clear disproportionate short stature. (*F*) Sanger sequencing data on patients M1, M2, F1, and F2, and the tested unaffected family members. The unaffected brother (III-3) and unaffected maternal half-brother (III-5) of patient F1 do not carry the variant. The *C1GALT1C1* c.59C>A variant is marked by a red box. Both male patients carry the variant hemizygously, the mother is heterozygous. (*G*) Pedigree. Black-filled symbols indicate affected *C1GALT1C1* c.59C>A hemizygous male patients, gray-filled symbols indicate affected heterozygous female patients. Individual IV-2 died on postnatal day three from kidney failure. Since no detailed clinical information was available, this individual has not been marked as affected by *COSMC*-CDG. Genotype information is indicated to the left of the respective symbol. Individuals without genotype information were unavailable for genetic testing.

changes in his blood count (asymptomatic thrombocytopenia [108,000/μL]). He also shows disproportionate short stature (height: 138 cm [<P1, −6.7Z]; *SI Appendix*, Fig. S1). Growth hormone deficiency was excluded in childhood. He has facial dysmorphisms with a high forehead, wide nasal bridge, short philtrum, retrognathia, prominent nasolabial folds, and posteriorly rotated ears (Fig. 2 *D* and *E*).

At the age of 21, patient M2 experienced an episode of severe AKI (maximum serum creatinine 2.3 mg/dL, urinary albumin/creatinine ratio 471 mg/g) with laboratory signs of TMA [schistocytosis, hemolytic anemia and severe thrombocytopenia (14,000/μL)]. He additionally showed elevated serum lipase levels in accordance with a HUS with accompanying acute pancreatitis. Complement analysis showed mild complement activation [complement component C3d: 60 mU/L (Ref. <40 mU/L), terminal complex sC5b-9: 232 ng/mL (Ref. 58 to 239 ng/mL)]. Based on our experience treating his younger half-brother, weekly Eculizumab treatment was initiated on day 4 after first presentation and normalized kidney function and serum lipase levels within 28 and 33 d, respectively, whereupon Eculizumab was discontinued. Patient M2 remains in stable remission with only persisting moderate proteinuria at his most recent follow-up, 4 mo after Eculizumab discontinuation (urinary albumin/creatinine ratio 200 mg/g). A kidney biopsy at this time showed no signs of persistent renal thrombotic microangiopathy, and only slight endothelial activation (*SI Appendix*, Fig. S2).

A maternal half-brother from a third partnership (Fig. 2*G*) developed renal failure and died 3 d after birth, but no autopsy was performed and no tissues were available for genetic analysis.

Patient F1 is the mother and patient F2 is the maternal grandmother of patients M1 and M2. Both patients F1 and F2 have borderline short stature and learning disability. The patients have a high forehead, retrognathia, prominent nasolabial folds and downturned corners of the mouth (Fig. 2*A*). During the birth of patient M2, patient F1 developed mild thrombocytopenia (90,000/μL) and anemia (10.5 g/dL), but has since had repeated normal blood results including differential blood counts. Patient F2 had slight thrombocytopenia when last examined (144,000/μL); she also suffers from chronic obstructive pulmonary disease and stage two chronic kidney disease (eGFR 62 mL/min/1.73 m^2) of unknown etiology. We detected no other organ dysfunction.

For additional clinical details, see the *SI Appendix*.

Genetic Testing. Conventional karyotyping, chromosomal microarray, and testing for fragile-X syndrome were normal in patient M1. Whole exome sequencing on venous blood from patients M1 and F1 identified no known genetic cause of the patients' phenotype, but detected the hemizygous variant c.59C>A (p.Ala20Asp) in *C1GALT1C1* in patient M1, carried heterozygously by patient F1. The variant segregated with the phenotype in the family (Fig. 2 *F* and *G*). Based on the extensive literature surrounding *C1GALT1C1* and the phenotypically similar mouse models, further functional studies were initiated.

Analysis of X-inactivation in whole blood of the two heterozygous female patients, where the a priori expectation would be that 50% of the cells express the mutant allele, instead showed a skewed X-inactivation pattern in both, with the wild-type allele preferentially inactivated. The allele carrying *C1GALT1C1* c.59C>A was active in 78.7% ± 7.2% of cells in the younger patient F1, and in

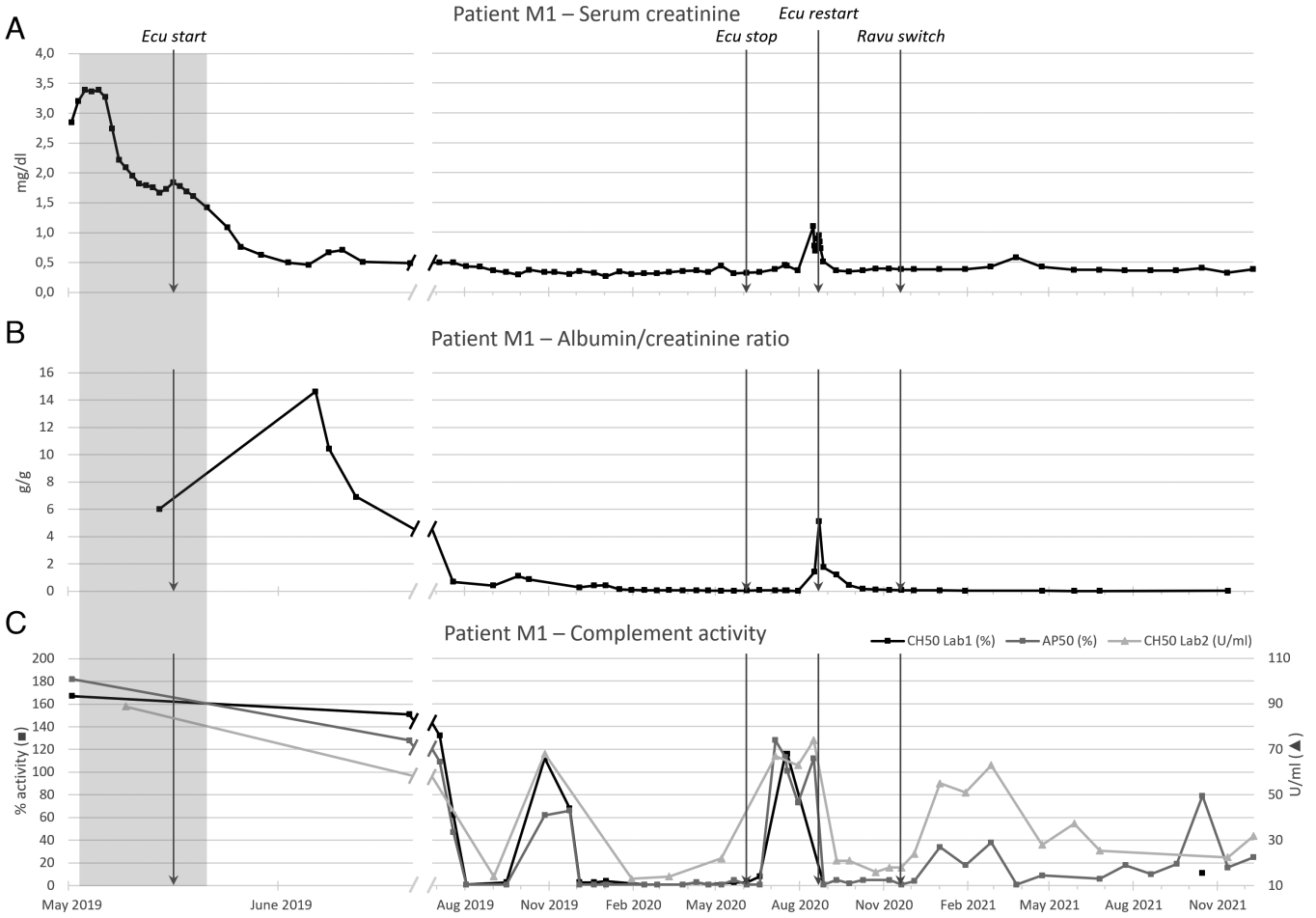

Fig. 3. Serum creatinine (*A*), urinary albumin/creatinine ratio (*B*) and complement activity (*C*) for patient M1 over 2 y starting at the initial presentation of AKI. Complement activity was measured in two laboratories with different CH50 assays. Laboratory 1 reported CH50 in percent activity, laboratory 2 in U/mL. After September 2020, samples were no longer regularly analyzed by laboratory 1. Peritoneal dialysis was performed during the gray-shaded time period. Initial incomplete suppression of complement activity was due to an increased urinary Eculizumab loss and difficulties in dosage finding. In November 2020, biweekly Eculizumab treatment was switched to four-weekly Ravulizumab infusions. AP50: alternative complement pathway activity; CH50: classical complement pathway activity; Ecu: Eculizumab; Ravu: Ravulizumab.

89.2% ± 0.7% of cells in the older patient F2 (mean ± 95% CI; analysis done in triplicate).

Characterization of Ala20Asp-Cosmc (A20D-Cosmc) and Glycosylation Analysis of Patient Cells.

Abundance of A20D-Cosmc variant is markedly reduced, leading to very low T-synthase activity. The A20D mutation occurs within the predicted transmembrane domain of Cosmc (Fig. 1*B*). To investigate A20D-Cosmc and its potential impact on O-glycans, first, we prepared EBV-immortalized lymphoblastoid cells from patients (M1 and M2) and healthy control (HC). Using these cultured cells together with other control cell lines (*Cosmc*-KO SimpleCell (25) and Jurkat, both of which lack Cosmc, and wild-type HEK293 cells), we analyzed the steady-state level of Cosmc and T-synthase proteins using SDS-PAGE western blot. Notably, we detected Cosmc protein only in positive controls (HC and HEK), but not in the male patient lymphoblastoid or *Cosmc*-KO cell lines. We also observed substantially reduced amounts of T-synthase in patient cells compared to the healthy control (Fig. 4*A*), consistent with our prior general deletion of *Cosmc* in mice and observation in cell lines (9, 26). In a parallel T-synthase assay, we found markedly reduced activity in lymphoblastoid cell lines of both male patients to <5% compared to the healthy control (Fig. 4*B*). The residual T-synthase activity indicates that a small amount of functional Cosmc is present in the lymphoblastoid cells of these patients, albeit at a very low level and likely below the detection limit of our immunoblot method. As a control, we measured the activity of hexosaminidase, another glycogene-encoded enzyme, but observed no significant differences between samples (Fig. 4*C*).

We next used wild-type Cosmc to rescue T-synthase activity, in which we transiently transfected the patient lymphoblastoid cells, as well as control Cosmc-deficient SimpleCells, with wild-type Cosmc and measured T-synthase activity in the lysates. The result showed a partial rescue of T-synthase activity in the studied cells (Fig. 4*D*).

To further investigate expression of A20D-Cosmc, we generated a tagged version of full-length forms of both A20D-Cosmc and wild-type (A20D-Cosmc-HPC4 and Cosmc-HPC4), transiently transfected these into SimpleCells, and analyzed whole cell lysates on SDS-PAGE immunoblot probed for the HPC4. The A20D-Cosmc-HPC4 showed substantially lower expression compared to wild type (Fig. 4*E*). Furthermore, we tested whether the recombinant A20D-Cosmc-HPC4 can restore the T-synthase activity by utilizing whole cell lysates prepared as in Fig. 4*E* together with lysates prepared from HEK cells, and assayed for their respective T-synthase activities. Our results demonstrate that A20D-Cosmc-HPC4 can partially rescue the loss of T-synthase activity (Fig. 4*F*). The expressed tagged Cosmc (Fig. 4*F*, "HPC4" and "Cosmc" rows) and a small amount of restored T-synthase protein are shown (Fig. 4*F*,

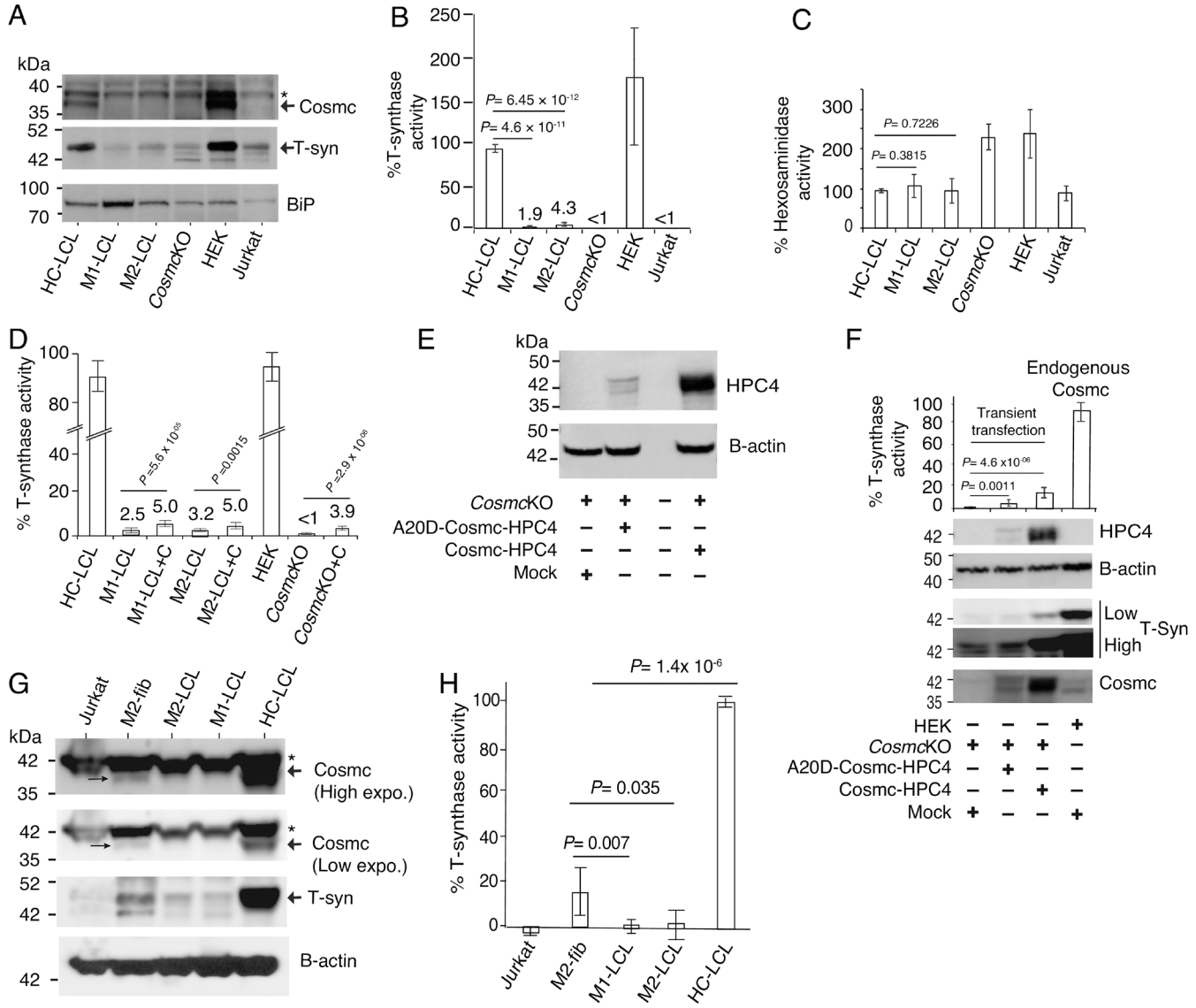

Fig. 4. A20D-Cosmc expression and its chaperone function on T-synthase activity. (*A*) Whole-cell lysates from cultured lymphoblastoid cells were analyzed by SDS-PAGE western blot, and probed for endogenous Cosmc, T-synthase, and BiP (loading control). (*B*) Similar to *A*, whole-cell lysates were assayed for T-synthase activity (n = 9, three independent experiments of n = 3). (*C*) As in *B*, hexosaminidase activity was measured (n = 12, three independent experiments of n = 4). (*D*) Wild-type *C1GALT1C1* (+C) partially rescues T-synthase activity in the patients' cells and control cell line (CosmcKO). Lysates were analyzed for T-synthase activity (n = 12, three independent experiments of n = 4). (*E*) Expression of A20D-Cosmc. Whole-cell lysates from transiently transfected cells as indicated on the bottom were analyzed by SDS-PAGE-WB, and probed as indicated (n = 3, a representative example). (*F*) In vitro expression of transiently transfected A20D-Cosmc-HPC4 can generate functional T-synthase. T-synthase activity from whole-cell lysates was measured (n = 9, three independent experiments of n = 3). Additionally, the same preparation of the lysates was analyzed by SDS-PAGE-WB and probed for the expression of A20D-Cosmc, B-actin, WT-Cosmc and T-synthase as indicated (n = 3, representative example). (*G*) Detectable level of endogenous A20D-Cosmc expression in M2 fibroblasts (M2-fib). Whole-cell lysates as shown, analyzed using SDS-PAGE-WB, and probed for endogenous Cosmc and T-synthase as indicated. Arrow (*Left*) shows A20D-Cosmc. Representative examples of n = 2. (*H*) Whole-cell lysates prepared as in G were analyzed for T-synthase activity (n = 6, two independent experiments of n = 3). HPC4, tagged Cosmc. *Cosmc*KO: *Cosmc*-knockout SimpleCells, Jurkat: Jurkat T lymphocyte-derived cancer cell line without endogenous Cosmc expression, HEK: HEK-293 human embryonic kidney cell line with high endogenous Cosmc expression. Lymphoblastoid cells: Healthy control (HC) and male patients (M1 and M2). Fibroblasts: M2-fib. Error bars represent ±SD. *nonspecific bands.

"T-Syn" rows). As an additional control, based on the presence of the *C1GALT1C1* c.58G>A (p.Ala20Thr) allele in the gnomAD database of human variation, we generated an A20T-Cosmc-HPC4 construct. We similarly tested A20T-Cosmc for expression and chaperone function. The A20T-Cosmc variant was functional and well expressed, and was able to rescue T-synthase activity (*SI Appendix*, Fig. S8), in line with this substitution being a benign variant.

We also studied different cell types from the same patients to see whether there are any differential impacts on expression of endogenous A20D-Cosmc. Interestingly, in our analysis on whole cell lysates of cultured fibroblasts from patient M2, we found that fibroblasts exhibited a higher level of A20D-Cosmc expression when compared to patient lymphoblastoid cells, but still substantially lower compared to control cells (HC) (Fig. 4*G*, Cosmc higher exposure, thin black arrow). We also tested whether the higher expression of A20D-Cosmc in M2-fibroblasts compared to cultured lymphoblastoid cells might lead to a higher abundance of T-synthase protein as well as increased activity. As might be expected, we observed a substantially higher amount of T-synthase protein present specifically in M2 fibroblasts (Fig. 4*G*, "T-syn" row) as well as higher T-synthase activity compared to lymphoblastoid cells (Fig. 4*H*). Consistent with this finding, we also observed similar results with M1 patient fibroblasts (*SI Appendix*, Fig. S3 *A* and *B*).

We next studied the possibility that the low steady-state abundance of A20D-Cosmc might be due to degradation by the proteasome-dependent pathway. To investigate this, we transiently transfected A20D-Cosmc-HPC4 into SimpleCells and treated the cells with or without Lactacystin, a proteasome inhibitor, and analyzed the lysates on SDS-PAGE immunoblot probed for the HPC4 tag. Interestingly, Lactacystin-treated samples showed significant accumulation of the A20D-Cosmc-HPC4 compared to mock treatment (*SI Appendix*, Fig. S7 *A* and *B*, *Top* row), suggesting that A20D-Cosmc is degraded by the proteasome pathway. As a control for proteasome-mediated degradation, in parallel, we also analyzed T-synthase which we found to be accumulated (*SI Appendix*, Fig. S7, *Bottom*, A and B), consistent with our previous findings (26).

These results indicate that the expressed A20D-Cosmc is functionally active, but the limiting factor is its lower amount due to degradation at least in part by the proteasomal pathway. Taken together, these results indicate that the A20D-Cosmc variant leads to a reduced abundance of both Cosmc and T-synthase expression in a cell-type–specific and tissue-specific manner, specifically impairing T-synthase activity.

Amount of A20D-Cosmc expression defines the truncated O-glycans in patients. To investigate O-glycan structures generated by A20D-Cosmc, we used ReBaGs6, an antibody specific for Tn-antigen (27), in flow cytometry with peripheral blood mononuclear cells (PBMC; all patients) and lymphoblastoid cells (hemizygous male patients). The Tn-antigen was expressed above unstained baseline in all patient cells, but not in the healthy control (Fig. 5 *A* and *B*). We further characterized O-glycans on lymphoblastoid cells using peanut agglutinin [PNA, a lectin that binds to T-antigen (28)], with or without neuraminidase (NeuA) treatment to remove sialic acid and expose potential underlying T-antigen. The lymphoblastoid cells of the male patients were stained by PNA, but less than the healthy control. There were no significant changes between cells of either patients or healthy controls when analyzed after neuraminidase treatment (Fig. 5*B*). As a control of other types of glycosylation, such as N-glycosylation, we observed no differences between the patient or control cells in binding by the lectin ConA, which binds broadly to many types of N-glycans (29) (Fig. 5*C*).

Next, we analyzed whole lysates from cultured lymphoblastoid cells of both male patients using SDS-PAGE western blots, and probed for both truncated and normal O-glycan structures as described above. Our analysis showed, in general agreement with the flow cytometry results, an increased expression of the Tn-antigen on glycoproteins from patient cells. In a parallel experiment, the presence of the normal T-antigen on patient cells was supported by specific binding with PNA lectin, indicating that the normal core 1 O-glycan is present in the male patients (Fig. 5 *D*–*F*).

A20D-Cosmc partially rescues the O-glycophenotype. We also investigated cell surface O-glycans on patient cells by transiently transfecting wild-type Cosmc similar to Fig. 4*D* and used flow cytometry analysis to characterize Tn-antigen expression using ReBaGs6 antibody as described above. Our results demonstrate that such transient transfection of Cosmc can result in partial reduction of Tn-antigen (Fig. 5*H*). We did not see any appreciable changes in the increase of normal core 1 O-glycans (Fig. 5*H*), likely due to the preexisting large amount of normal O-glycans in the patient cells. On the other hand, we asked whether transient transfection of A20D-Cosmc in SimpleCells could partly restore T-synthase activity (Fig. 4*F*), and reduce the expression of Tn-antigen. The SDS-PAGE-WB analysis probed with ReBaGs6 demonstrates a partial reduction of Tn-antigen expression (*SI Appendix*, Fig. S4, mock vs. others), and indicates, in parallel with Fig. 4*F*, that A20D-Cosmc at a higher abundance can reduce expression of the Tn-antigen. Furthermore, to gain deeper insights into the O-glycophenotype in the context of the A20D-Cosmc variant, we used M2 fibroblasts which contain a detectable level of endogenous A20D-Cosmc and produce a substantial amount of active T-synthase compared to lymphoblastoid cells (Fig. 4 *G* and *H* and *SI Appendix*, Fig. S3 *A* and *B*). Our result shows that the reduced level of A20D-Cosmc present in the M2 fibroblast is still functional as the fibroblasts express normal O-glycans (*SI Appendix*, Fig. S5 *A*, *B–D*, *Bottom*), and by western blot, no clearly detectable level of Tn-antigen could be observed (*SI Appendix*, Fig. S5*B*). Consistent with the above results, however, the lymphoblastoid cells from both patients express the Tn-antigen, though in variable amounts. As a control, detection of the Tn-antigen by ReBaGs6 can be specifically inhibited by the hapten GalNAc, but not by the control isomer GlcNAc (*SI Appendix*, Fig. S5 *D* and *C*). We also observed similar results when analyzing M1 fibroblasts (*SI Appendix*, Fig. S5*E*).

Additionally, we analyzed cell surface O-glycan expression on patient M2 fibroblasts, using flow cytometry, as described above in the case of lymphoblastoid cells. Our result showed that M2 fibroblasts lack expression of the Tn-antigen as compared to lymphoblastoid cells (*SI Appendix*, Fig. S6 *A* and *B*). Together, these results suggest that the level of A20D-Cosmc expression, which is different between fibroblasts and lymphoblastoid cells, determines the O-glycophenotype in these patients and that it likely differs between other cell populations in vivo.

Increased levels of serum Gd-IgA1. One important phenotypic feature in the male patients was AKI. Previous studies suggest that defects in Cosmc and T-synthase in IgA1-producing B-cells may lead to expression of galactose-deficient IgA1 (Gd-IgA1) (17, 30). This modification plays a central role in the pathogenesis of IgA nephropathy (19, 31–34). We therefore tested the serum of all four patients and of healthy controls for Gd-IgA1 using VVA lectin (recognizes Tn-antigen) and for IgA1 with normal core 1 O-glycans using PNA lectin. Interestingly, we found that all patients show high levels of VVA binding indicative of Tn-antigen expression in IgA, indicating high expression of the Gd-IgA1 glycoform, but no detectable core 1 O-glycosylated IgA1, which was observed in control sera (Fig. 5*G*).

Discussion

Here we report the identification of four patients from one family, two hemizygous males and two heterozygous females, carrying the c.59C>A (p.Ala20Asp) missense variant in the X-chromosomal *C1GALT1C1* gene. We show this variant to be causative for *COSMC*-CDG, a novel chaperonopathy that leads to a multisystem disorder of O-glycosylation. While the males presented with a severe multisystem phenotype, the females exhibit less pronounced clinical phenotypes in line with X-linked semidominant inheritance. The combination of thrombocytopenia, immune deficiency, developmental delay, short stature, facial dysmorphisms and variable-onset acute kidney injury resembling aHUS in hemizygous males likely represents a clinically recognizable phenotype. We also present a deep biochemical characterization of the A20D-Cosmc variant and the O-glycans generated by this variant. Our results show that the tissue-variable expression level of A20D-Cosmc defines the respective cellular O-glycophenotype in male patients.

COSMC-CDG is remarkable in that it negatively affects the rate-limiting step in the O-glycosylation pathway, i.e., the formation of the core 1 O-glycan. This step is not only necessary for extended and mature O-glycan expression, but also exclusively performed by a single enzyme, the T-synthase. T-synthase can only function when its specific chaperone Cosmc is also expressed.

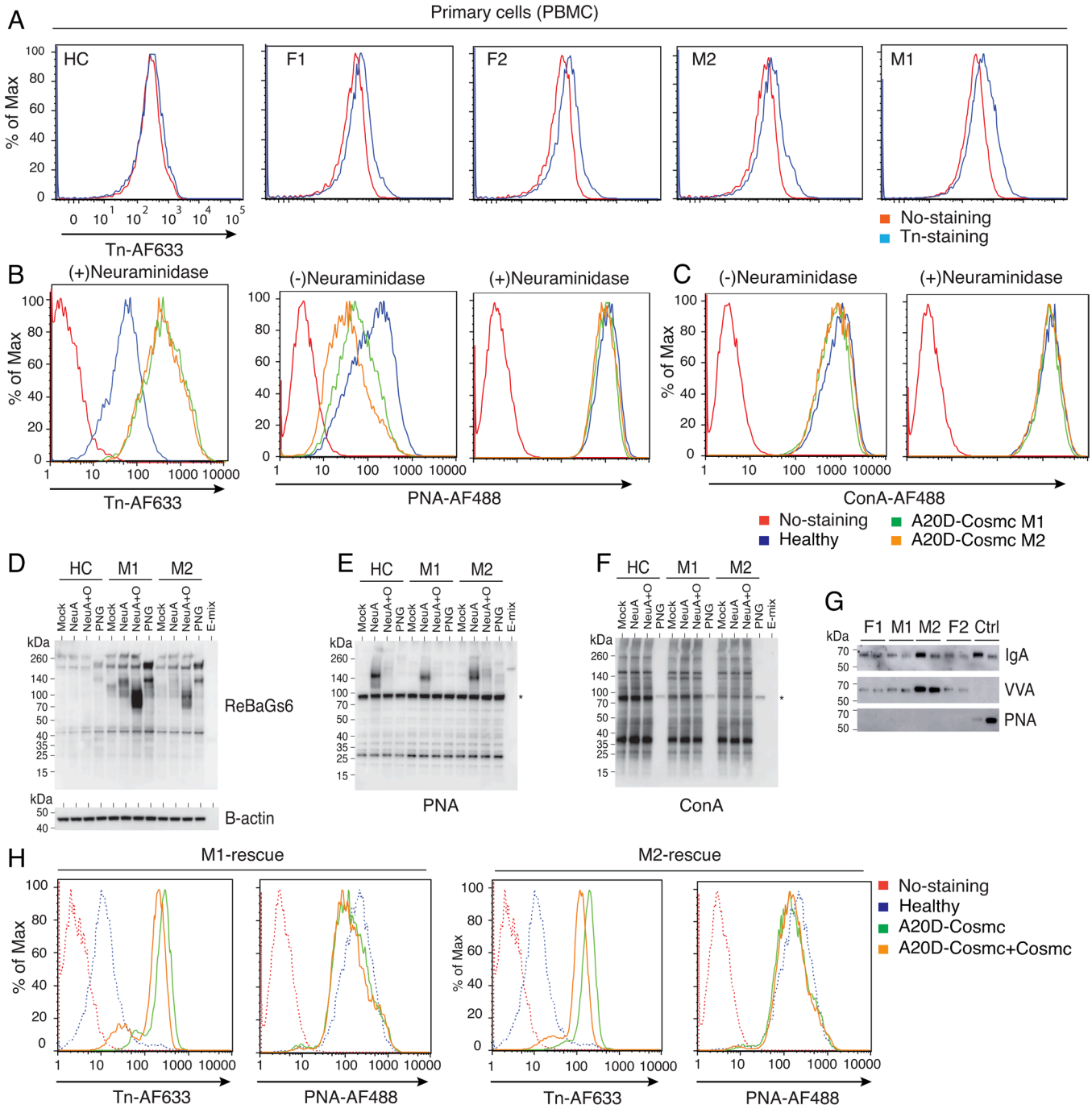

Fig. 5. Characterization of cell surface and total O-glycans from A20D-Cosmc patients' cells. (*A–C*) Primary PBMCs (panel *A*) and cultured lymphoblastoid cells (panels *B* and *C*) from healthy control (HC), both female patients (F1 and F2), and both male patients (M2 and M1) as indicated, analyzed for their surface glycan expression as indicated (ReBaGs6 antibody [binds to truncated O-glycan, Tn-antigen], PNA lectin [binds to normal O-glycan, T-antigen], ConA lectin [N-glycans, binds to mannosylated glycans]) using flow cytometry. For the analysis of sugar structures, cells were first treated with mock or neuraminidase. FACS plots for A (n = 1)/FACS plots for B (n = 3), *P* values: $P = 0.0404$ (M1 vs. healthy), $P = 0.0283$ (M2 vs. healthy); and normal O-glycans expression measured by PNA, without Neuraminidase (n = 3), *P* values: $P = 0.2094$ (M1 vs. healthy), $P = 0.0981$ (M2 vs. healthy); with Neuraminidase (n = 3), *P* values: $P = 0.2919$ (M1 vs. healthy), $P = 0.3962$ (M2 vs. healthy). (*C*) For normal N-glycans expression (n = 2), without Neuraminidase, *P* values: $P = 0.0983$ (M1 vs. healthy), $P = 0.2239$ (M2 vs. healthy); with Neuraminidase, *P* values: $P = 0.1402$ (M1 vs. healthy), $P = 0.4183$ (M2 vs. healthy). (*D–F*) Glycan characterization on whole-cell extracts. Similar to Fig. 4*C*, whole-cell extracts were prepared and treated with neuraminidase (NeuA, removes sialic acid), NeuA and O-glycosidase (NeuA+O, removes non-sialylated T-antigen), PNGase-F (PNG, removes all N-glycans), or untreated (Mock). The preparations and enzyme mixture (E-mix) were resolved on an SDS-PAGE gel. B-actin serves as a loading control. Blot images are one of the representative images of three independent experiments. Asterisk (*) indicates nonspecific binding from HRP-streptavidin. (*G*) Characterization of IgA1. Serum from patients and pooled healthy control were used to purify total IgA and treated with mock (left lane under each respective sample heading) or Neuraminidase (right lane). SDS-PAGE-WB/LB were used to probe for total IgA, Gd-IgA1 (VVA lane), and IgA1 with normal O-glycans (PNA lane). All patients have high levels of Gd-IgA1, but no normally O-glycosylated IgA1 (bottom, PNA stain). Control normally O-glycosylated IgA1 is stained by PNA after removal of sialic acid by Neuraminidase (PNA, last lane). Representative example of three independent experiments. (*H*) Transient transfection of wild-type Cosmc on patient cells reduces expression of the immature Tn-antigen, partially restoring normal O-glycosylation. Flow cytometry analysis was performed similar to *A*, on cells treated with neuraminidase. FACS plot for H (n = 3), M1 rescue, Tn antigen expression, *P* value = 0.0258 (M1 vs. M1+Cosmc) and Normal O-glycans expression measured by PNA, *P* value = 0.5053 (M1 vs. M1+Cosmc); similarly, for M2 rescue, Tn antigen expression, *P value* value = 0.0416 (M1 vs. M1+Cosmc) and Normal O-glycans expression measured by PNA, *P* value = 0.3051 (M1 vs. M1+Cosmc).

Based on the lethal phenotype of complete *Cosmc* knockout in mice and the critical function of T-synthase in O-glycosylation, we had earlier assumed that in humans, a complete loss of Cosmc function would not be compatible with life. Of the 51 large deletions encompassing *C1GALT1C1* in the human mutation databases ClinVar and DECIPHER, all occurred heterozygously in females. In line with this assumption, our functional studies of A20D-Cosmc cell lines show a substantial, but not complete reduction of T-synthase activity, and A20D-Cosmc itself was expressed at significantly reduced levels. The A20D-Cosmc expression was higher in patient fibroblasts than in lymphoblastoid cell lines. A complete loss of Cosmc function leads to an effectively complete loss of T-synthase function, as evident from *C1galt1c1*-KO mice and *C1GALT1C1*-KO human cell lines (9, 25). The residual T-synthase activity in cell lines from our patients therefore strongly suggests that the chaperone function of the A20D-Cosmc is not fully abrogated, and the low expression of the protein can significantly, but not completely, function to effect the correct folding of the T-synthase. This conclusion is also supported by our experiments transfecting cells without any endogenous Cosmc and T-synthase activity (SimpleCells) with A20D-Cosmc, leading to a partial restoration of both T-synthase protein and activity.

We found evidence that A20D-Cosmc is degraded by the proteasomal machinery which may explain the reduced steady-state level of A20D-Cosmc expression in patient cells. However, we cannot currently exclude other additional mechanisms leading to the observed dramatic loss of A20D-Cosmc expression. Taken together, rather than an impaired chaperone function, we demonstrate that the primary pathomechanism of A20D-Cosmc is a reduced protein abundance.

Transient transfection of patient cells with functional Cosmc was able to partially restore T-synthase function and thereby partially rescue the biochemical phenotype. While immature Tn-antigen was detectable in all patients, we saw that the majority of glycoproteins nonetheless showed normal O-glycosylation - even in the hemizygous male patients. This indicates a substantial functional reserve of T-synthase activity in healthy individuals. It remains unclear at present why the levels of T-synthase activity and Tn-antigen are measurably different between the two hemizygous half-brothers harboring the identical missense variant (Figs. 4 and 5). Since the immunological phenotype has ameliorated with age in the older half-brother, this difference may be age-related or due to environmental factors.

Of particular interest was the manifestation of AKI in both male patients. Following the preprint publication of our findings on Research Square, a single case report of a patient carrying a de novo hemizygous missense variant (c.266C>T; p.T89I) in *C1GALT1C1* was recently published (11). This patient is reported to have short stature, speech developmental delay, neutropenia, thrombocytopenia and also presented with acute kidney injury at the age of two weeks. This patient's episode of AKI was clinically diagnosed as aHUS and, as in our patients, proved responsive to treatment with Eculizumab.

Increased levels of circulating Gd-IgA1, likely caused by clonal loss-of-function of T-synthase or the Cosmc chaperone in IgA-producing plasma cells (30, 35), represent the initial step in the multi-hit pathomechanistic model of IgA nephropathy, the most common form of primary glomerulonephritis worldwide (17, 30–32, 34). Interestingly, we observed very high levels of Gd-IgA1 in both the hemizygous males and the heterozygous females. Unexpectedly, there was a complete lack of staining by PNA, which binds normal core 1 O-glycans of IgA1. This is an unpredicted observation in the female patients, likely explained by a skewed X-inactivation in IgA-producing plasma cells as indicated by the patients' strongly skewed X-inactivation in blood. Somatic loss-of-function of Cosmc is also a hallmark feature in the majority of human carcinomas (24), and a clonal selective advantage for cells with deficient O-glycosylation has been proposed (36). This is consistent with our observation of skewed X-inactivation in favor of the mutant *C1GALT1C1* allele in the hematopoietic system of heterozygous females.

Taking into account the mostly unremarkable kidney biopsy of patient M2 after complete clinical remission of his acute kidney injury, the role of Gd-IgA1 in *COSMC*-CDG-associated nephropathy remains unclear at present. The initial episode resembling renal thrombotic microangiopathy may have been triggered by an IgA nephropathy-like pathomechanism, i.e., the production of anti-Gd-IgA1 antibodies [as is thought to happen in classic IgA nephropathy (37, 38)]. Lacking kidney sections from the active phase of the *COSMC*-CDG-associated nephropathy, prior to therapeutic intervention, this hypothesis is currently untested. However, the clinical presentation of IgA nephropathy patients with a thrombotic microangiopathy phenotype has been previously reported (37). We also note that anti-C5 antibody treatment with Eculizumab has been efficacious in single case reports of patients suffering from biopsy-confirmed IgA nephropathy (39), probably by suppressing anti-Gd-IgA1/Gd-IgA1-immunocomplex-dependent complement-mediated renal inflammation (40, 41). Since the factors leading to the production of anti-Gd-IgA1 antibodies are currently unknown, the evidence discussed above leads us to speculate that patients with *COSMC*-CDG are at an increased risk for IgA nephropathy. Additionally, podocyte-specific conditional *C1galt1c1*-knockout mouse models show proteinuria and focal segmental glomerulosclerosis (42), suggesting a deleterious effect of impaired O-glycosylation directly in the podocyte. In our opinion, the episodic relapsing course of the nephropathy with complete remission under complement inhibition therapy is not easily explained by an inherent podocytic defect alone. As such, we regard the *COSMC*-CDG-associated nephropathy as likely multifactorial with a predominant triggered immunological component as well as an inherent podocytic defect. Future studies will hopefully shed more light on this aspect.

Both hemizygous male patients showed clinical and hematological evidence of a severe immunodeficiency with neutropenia, lymphopenia and hypogammaglobulinemia. Some of these features have been noted in patients with Tn syndrome (*SI Appendix*, Table S2), resulting from a somatic mutation of *C1GALT1C1* in hematopoietic precursor cells (22), and in mice with targeted deletion of *C1galt1c1* in endothelial/hematopoietic cells and B cells (43). Thus, these features are consistent with evidence that O-glycans are critical for normal leukocyte trafficking, antibody production, and cellular turnover. Most recently, mice with an inducible global knockout of *C1galt1c1* notably showed leukopenia, thrombocytopenia, acute kidney failure, gastric ulcers and acute pancreatitis (44), leading to a high mortality. With the exception of gastric ulcers, each of these clinical features have presented in our patients at different timepoints.

In conclusion, we have delineated a novel X-linked congenital disorder of glycosylation involving core 1-based O-linked glycosylation, which we propose to term *COSMC*-CDG. This is caused by subtotal loss-of-function of Cosmc, the specific chaperone for the formation of active T-synthase, thus leading also to a loss of T-synthase activity. In the course of treating these patients, we identified inhibition of complement component C5 as an efficacious treatment for the disease-associated AKI, likely preventing further progression of renal disease in two patients. Finally, studying this novel *COSMC*-CDG functionally has advanced our understanding of basic glycobiology and the roles of O-glycans in biological processes.

Materials and Methods

Ethics Approval. This study was approved by the Ethics Committee of the medical faculty of the University of Cologne (ID 15-215). All adult probands and the legal guardians of minors gave written informed consent for study participation and the publication of clinical and experimental data, as well as photographs. Blood samples of healthy controls were collected at the Beth Israel Deaconess Medical Center under an IRB-approved protocol (ID 2016P000008). This research conforms to the Helsinki Declaration of ethical principles for medical research involving human subjects.

Whole-Exome Sequencing. For whole-exome sequencing library preparation, we used the Nextera Rapid Capture Exome (v1.2) according to the manufacturer's protocol (Illumina). Sequencing was performed on a NextSeq500 Sequencer with 2 × 75 cycles. Variant annotation and filtering was done in the exome and genome analysis pipeline "Varbank2, varpipe v3.4" (45) of the Cologne Center for Genomics (University of Cologne).

We performed Sanger confirmation of the detected *C1GALT1C1* variant in all probands.

Variant Reporting. Variant reporting refers to the *C1GALT1C1* transcript NM_152692.5 in the human hg19 genomic reference. The variant has been submitted to the ClinVar variant database (accession ID VCV001675199.1).

X Inactivation Assay. One microgram of genomic DNA samples isolated from peripheral blood was predigested with 20 units of the methylation-sensitive restriction endonuclease HpaII (New England Biolabs) in a total reaction volume of 20 µL, and incubated at 37 °C for 12 h. The enzymatic reaction was stopped by heating the mixture to 80 °C for 20 min. PCR amplification of the *SLITRK4* locus was performed using 100 ng (from females) or 200 ng (from males) undigested or HpaII-digested DNA in a total reaction volume of 20 µL containing: Qiagen Multiplex 5 µL, 0.5 µmol/L FAM-labeled forward *SLITRK4* primer (5′-GCACACAAGCAGTCCTTCCT-3′), 0.5 µmol/L reverse *SLITRK4* primer (5′-TGGCTTCTTGGTTGCTCTCT-3′), and 2 µL Q-solution. Amplification was performed under the following conditions: 1 cycle for 12 min at 94 °C; 35 cycles for 30 s at 95 °C, 30 s at 72 °C, and 1 min at 60 °C; 1 cycle for 60 min at 60 °C.

PCR products were analyzed on an ABI 3100er genetic analyzer (Applied Biosystems) using Certagen LS-600-ORN as an internal-lane size standard and GeneMapper software (Applied Biosystems). The X-inactivation ratios were calculated as previously described (46).

Complement Activity Assay. Complement activity analysis and Eculizumab treatment monitoring were performed according to previously published protocols (47).

Kidney Biopsy Staining. The renal biopsy was processed according to standard protocols for renal biopsy diagnostics. Immunohistochemical staining were performed on formalin-fixed paraffin-embedded material after deparaffinization and rehydration (1-µm sections). Antigen retrieval was performed with pronase E digestion (Sigma Aldrich). Primary antibodies included rabbit polyclonal antibodies against C3c (A0062; DAKO Deutschland), C5b-9 (M0777; DAKO Deutschland), IgA (A0262; DAKO Deutschland) and IgM (A0425; DAKO Deutschland).

Generation of Studied Cell Lines. Lymphoblastoid cell lines were generated from venous blood samples of patients M1, M2, F1, and F2, and from a healthy control. Blood samples were processed within 2 h of collection. In a 50 mL Falcon tube, approximately 5 mL of venous blood and 45 mL of erythrocyte lysis buffer were agitated, incubated for 10 min at room temperature, and centrifuged for 10 min at 3,000 *g*. The supernatant was discarded and the remaining pellet resuspended in lysis buffer. This process was then repeated and the resulting cell pellet resuspended in 2 mL of culture medium containing EBV virus particles. The suspension was then incubated at 37 °C at 5% CO_2 for 1 h and filled up to 5 mL in a T25 culture flask with RPMI 1640 medium supplemented with 20% FCS, Penicillin/Streptomycin, Amphotericin B and cyclosporine (2 µg/mL). The culture flask was placed into the incubator at 37 °C at 5% CO_2. The B lymphoblastoid cell culture was expanded over several weeks while exchanging the growth medium weekly at first, and every 3 d once cells had sufficiently expanded to form clearly visible cell clusters. For long-term storage, cell cultures were centrifuged for 5 min at 240 *g*, pellets resuspended in a mixture of 90% fetal bovine serum and 10% DMSO culture medium, and then frozen to −80 °C at a rate of approximately 1 to 2 °C per minute.

Patient fibroblast cell lines were generated from an anterior chest skin sample obtained during cardiac surgery for membranous subaortic stenosis (patient M1), and a skin biopsy specimen of the left posterior forearm (patient M2) using standard protocols. The generation of patient M2's fibroblast cell line was performed at "CBC BioTec" (CRB-HCL, Hospices Civils de Lyon Biobank BB-0033-00046).

T-Synthase Activity Assay. One million cells [healthy controls, patients, *C1GALT1C1*-KO SimpleCell (25) cells, HEK cells and Jurkat cells] were cultured in six-well plates for 24 h. Cell lysates were prepared in 200 µL lysis buffer (50 mM Tris-HCl pH7.4, 150 mM NaCl, 1 mM EDTA, and 1% Triton X-100 containing protease inhibitors) for 5 min on ice. The lysates were then sonicated (amplitude 30, 5× for 1 s each) on ice. The supernatant was collected by centrifugation at 21,000 *g* for 10 min at 4 °C. Protein concentrations were determined using a BCA protein assay.

T-synthase activity measurement was performed as described previously (48). The highest picomoles/mg/h activity within replicates of an experiment was converted to 100% and utilizing the highest activity as 100%, the rest of the other activities are calculated. Every sample was analyzed in three to four replicates. Samples were mixed with T-synthase reagent on a chilled plate, and the assay was carried out at 37 °C for 50 min followed by placing on ice for 10 min. The reaction was stopped by adding 100µL cold 0.1M Glycine/NaOH pH9.6, and 4-methylumbelliferone (4-MU) fluorescence was measured immediately (excitation/emission: $355^{nm}/460^{nm}$) on an ImageXpress Pico (Molecular Devices).

Flow Cytometry. Approximately 1 million lymphoblastoid cells and 500,000 peripheral blood mononuclear cells (PBMC), respectively, from the patients and a healthy control were suspended in 100 µL or 50 µL of PBS and were then mock or neuraminidase [1 µL, Sialidase, Roche (Ref. 10269611001)] treated at 37 °C for 1 h. Cells were extensively washed with PBS and then incubated with 2 µg/mL biotinylated Peanut Agglutinin, PNA (Vector Laboratories #B-1075), biotinylated Concanavalin A, ConA (Vector Laboratories #B-1005), or 0.5 µg/mL biotinylated *Vicia villosa* lectin, VVA (Vector Laboratories #-1235) for 30 min on ice, washed again and stained with secondary streptavidin conjugated with Alexa Fluor-488 (1:500) for another 30 min on ice covered with aluminum foil. Similarly, anti-Tn antibody conjugated with Alexa Fluor-633 prepared in house (27) was incubated with the cells (1 µL of the antibody per 10^6 cells in 50 to 100 µL of PBS containing 0.5% albumin or fetal bovine serum (FBS), and 5% Human TruStain FcX™ in PBMCs) for 30 min on ice. The stained cells were washed twice with PBS and analyzed on a BD FACSCalibur (lymphoblastoid cells) or BD FACSCanto I (PBMCs) flow cytometer. Data analysis was performed using FlowJo and DIVA 5.0 software.

For comparison between patients lymphoblastoid and fibroblast cells, cells were stained as described above and analyzed on Attune NxT (Invitrogen).

Hexosaminidase Activity Assay. Approximately 5 µg of the lysate in 10 µL were incubated with 40 µL of reaction mixture containing 610 µM of 4MU-GlcNAc, 0.25% of Triton X-100 and 120 mM of cacodylate buffer pH 6.4 for 1 h at 37 °C. Stopping of the reaction and measurement of the 4-MU was done as described above. The highest picomoles/mg/h activity within four repeats of an experiment was converted to 100% for healthy control (HC) and accordingly for all others.

Transient *C1GALT1C1* Transfection. For transient transfection, 30 µg of wild-type human *C1GALT1C1* in a pGen2.1 vector (GenScript) or empty vector (diluted to 0.5 µg/µL in medium) was incubated with the cultured lymphoblastoid cells (approx. 2×10^6 in T25 flask) in 1 mL of fresh RPMI 1640 complete media (incubated at 37 °C and 5% CO_2) for 5 min. Eighteen microliters freshly prepared polyethylenimine (1 mg/mL in 25 mM HEPES, 150 mM NaCl, pH 7.5) (Cat#23966, Linear, MW 25,000, Polysciences, Inc.) was filtered at 0.22 µ and diluted to 0.5 mg/mL medium, and was added to the cultured cells. After 24 h, 5 mL of the fresh pre-warmed complete media supplemented with valproic acid (Cat#P4543, Sigma Aldrich) was added to a final concentration of 2.2 mM. In parallel, adherent SimpleCell (~1 million cells, cultured for 12 h) were transiently transfected. At 4 d post-transfection, 2 million cells were collected by centrifugation (400 *g* for 4 min) and washed twice with 1 mL chilled PBS. Cells were lysed immediately as described above. T-synthase activity was measured on day 4 post-transfection, and flow cytometry was performed on day 7 post-transfection.

Characterization of Glycan Expression. For immunoblots, lysates run on SDS-PAGE gels were transferred onto PVDF membrane by a wet-transfer system at 4 °C or Trans-Blot Turbo Transfer system (Biorad). The membranes were blocked with 5% non-fat milk in 1× TBST (50 mM Tris-HCl, pH 7.2, 150 mM NaCl

containing 0.05% tween-20) at RT for 1 h and incubated overnight with primary antibody diluted in 5% non-fat milk (1× TBST). This was followed by incubation with the horseradish peroxidase (HRP)-conjugated secondary antibody at 1:5,000 dilution in 5% milk in 1× TBST. The following dilutions of primary antibodies were used: anti-Cosmc (H-10, Santa Cruz #SC-271829, 1:1,000), anti-T-synthase (F31, Santa Cruz #SC-100745, 1:1,000), anti-BiP (Abcam, #ab108613, 1:2,000), and anti-β-actin (C4, Santa Cruz #SC-47778, 1:1,000). In the case of ReBaGs6 (an in-house murine recombinant anti-Tn-antigen IgM), the membrane was blocked with 5% BSA 1× TBST for 1 h at RT, then incubated overnight with 1 μg/mL of ReBaGs6 in 1% BSA 1× TBST, followed by HRP-labeled goat anti-mouse IgM (Jackson ImmunoResearch Laboratories, Inc. #115-035-020, 1:5,000) in 0.5% BSA 1× TBST for 1 h. For ReBaGs6 WB inhibition experiment, 100 mM GalNAc (Biosynth #MA04390) or control GlcNAc (Sigma #A8625) (prepared in 1× TBST+300 mM NaCl containing 1% BSA) with ReBaGs6 were added to prior blocked (5% BSA, 1× TBST) nitrocellulose membrane and proceed as defined above. Similarly, 100 mM Galactose (Sigma, #G-0750) and control 100 mM Glucose (Sigma, #G54000) were added to PNA blots. The signals were detected using an Amersham™ Imager 600 (GE Healthcare Life Sciences) using SuperSignal™ West Pico PLUS Chemiluminescent Substrate or SuperSignal® West Femto Maximum Sensitivity Substrate (Thermo Fisher Scientific).

For lectin blots, 100 μg lysate was boiled in 1× Glycoprotein denaturing buffer (NEB) for 10 min and treated with either mock or 1 μL of each enzyme: α2-3,6,8,9 Neuraminidase A (NeuA, Cat#P0722S), a combination of NeuA and O-glycosidase (Cat#P0733S), or PNGase F (Cat#P0708S) for 2 h at 37 °C following the manufacturer's protocol (NEB). Of this preparation, ~5 to 10 μg was then resolved and transferred onto PVDF/ nitrocellulose as described above. The membranes were blocked with 5% BSA in 1× TBST for 1 h at RT and incubated with the following biotinylated lectins: *V. villosa* Lectin (VVA, Cat#B-1235-2, diluted to 1 μg/mL), peanut agglutinin (PNA, Cat#B-1075-5, diluted to 0.5-2 μg/mL), Concanavalin A (ConA, Cat#B-1005-5, diluted to 0.1 μg/mL), diluted to 5 μg/mL) in TBST overnight at 4 °C. After washing twice with TBST for 5 min, the membranes were incubated with HRP-labeled streptavidin (Cat#SA-5014-1, Vector Laboratories) at 1:5,000 dilution for 1 h at RT, and the signals were analyzed as described above.

Purification of IgA from Human Sera. Ten microliters of human sera was first diluted with 90 μL of chilled 1x PBS, followed by incubation with 20 μL (50% slurry in PBS) of goat anti-human IgA (α chain) agarose beads (Sigma, Cat#A2691) overnight at 4 °C on a rotator (10 rpm). Bound materials were washed twice with 500 μL of cold 1× PBS, and eluted by 50 μL of 0.1 M glycine-HCl (pH 2.7) to the beads and neutralized. Protein concentration was determined by NanoDrop (A280).

O-Glycosylation Analysis on IgA by Western and Lectin Blot. Approximately, 0.3 μg of purified IgA was treated with either 1 μL of neuraminidase (Roche, #10269611001) or mock at 37 °C for 1 h. ~0.1 μg was analyzed on SDS-PAGE-WB. For IgA detection, the membrane was blocked with 5% (w/vol) non-fat milk in 1× TBST for 1 h, and incubated with HRP-labeled goat anti-human IgA (α chain) (Cat#5220-0360, KPL) antibodies at 1:2,000 in 1× TBST containing 1% non-fat milk for 1 h. After washing 3× with 1× TBST for 10 min each, the signals were analyzed as described above. VVA and PNA blots were performed as described above.

Generation of the A20D- and A20T-Cosmc-HPC4 Variants and Cosmc-HPC4 WT Constructs and Transient Transfections. Cosmc constructs containing the HPC4 tag (EDQVDPRLIDGK) C-terminally were generated using the mammalian pGen2.1 vector (GenScript). Cells were transiently transfected using *X-tremeGENE*™ HP DNA Transfection Reagent kit (Sigma-Aldrich). Briefly, 2 μg of plasmid or empty vector was mixed with the transfection reagents as specified by the company's protocol and transfected onto Cosmc deficient SimpleCells and HEK cells cultured in six-well plates (approximately 90% confluent) in DMEM medium containing Penicillin/Streptomycin, Amphotericin B, and Glutamine at 37 °C at 5% CO_2. After ~3 d of transfection cells were collected.

T-Synthase Activity Assay and Western Blot Analysis of the Transiently Transfected HPC4-Tagged Cosmc. Transiently transfected cells with A20D-Cosmc-HPC4 and other controls were collected (centrifugation, 400 *g*, 5 min) and washed with 1 mL of chilled PBS. Cells were lysed using 200 μL of Lysis buffer (50 mM Tris-HCl pH 7.4, 150 mM NaCl, 0.5% Triton X100, 1 mM $CaCl_2$, one protease inhibitor/10 mL) for 30 min (vertexing every 5 min) on ice followed by sonication (amplitude 39, 7× for ~2 s each). The supernatant was collected by centrifugation at 21,000 *g* for 15 min at 4 °C. For the T-synthase activity assay, freshly prepared lysates prepared directly after ~3 d of transfection were used and measured the activity as described above.

WB Analysis for HPC4-Tagged Protein. Nearly 80 micrograms of the whole-cell lysates from the transiently transfected cells described above was resolved using SDS-PAGE, and the resolved proteins were transferred to the nitrocellulose membrane as described above. The membrane was blocked for an hour with 5% non-fat milk (1× TBS + 1 mM $CaCl_2$) followed by incubation with HPC4 antibody (1.5 μg/mL) in the same blocking reagents overnight. After washing the membrane twice with TBS+1 mM $CaCl_2$ for 5 min, the membranes were incubated with HRP-labeled anti-mouse IgG at 1:5,000 dilution (5% non-fat milk in 1× TBS + 1 mM $CaCl_2$) for 1 h at RT. The membrane was washed five times with TBS + 1 mM $CaCl_2$, and the signals were analyzed as described above.

Culturing M1 and M2 Fibroblasts, HEK, SimpleCell, and Jurkat Cells. M2 patient fibroblasts, HEK, and SimpleCell were cultured in Dulbecco's modified Eagle medium (DMEM) containing 10% FCS, Penicillin/Streptomycin, Amphotericin B, and Glutamine; similarly, Jurkat cells were cultured in RPMI as described above. Whole-cell lysates were prepared as described in transiently transfected cells.

Proteasome Inhibition Experiment. Simple cells cultured in six-well plate (at 80 to 90% confluency) were transiently transfected with A20D-Cosmc-HPC4 and mock as described above. After 65 h of transient transfection, 5 and 10 μM Lactacystin (final concentration) or respective volume of DMSO was used and incubated for 6, 12, and 24 h (one plate for each time point). Cells were trypsinized and collected with 1ml of chilled PBS, pelleted (500 *g*), and washed once with 1 mL of PBS. Cell pellets snap frozen in dry ice and were lysed and processed at the same time. Lysates were quantified for protein concentration and stored at −20 °C. SDS-PAGE WB was performed as described above (WB analysis for HPC4-tagged protein). Western blot data were quantified using ImageJ. The highest value obtained in each time point was converted to 100% and the rest were normalized accordingly.

Data, Materials, and Software Availability. Source data for T-synthase/hexosaminidase activity graphs and flow cytometry graphs (Figs. 4 and 5) and *SI Appendix*, Figs. S3, S6, S7, and S8) are available herein (Dataset S1). Human whole exome sequencing data of the study participants cannot be made publicly available due to data protection regulations.

ACKNOWLEDGMENTS. We thank the study's participants for their willingness to contribute to this project. We also thank Aditya Ramanujan, Rachael Smith, and Camille M. Bucci for their technical assistance, and Jamie Heimburg-Molinaro for manuscript editing and review. This work was supported by the Deutsche Forschungsgemeinschaft (DFG, German Research Foundation) - Clinical research unit (KFO 329, AL901/2-1 and AL901/3-1) to J.A. and Clinical research unit (KFO 329, BE6072/2-1 and BE6072/3-1) to B.B.B. Further support by the Glycoscience Fund, BIDMC to R.D.C.

Author affiliations: [a]Institute of Human Genetics, University Hospital Cologne, Faculty of Medicine, University of Cologne, 50931 Cologne, Germany; [b]Center for Molecular Medicine Cologne, University of Cologne, 50931 Cologne, Germany; [c]Division of Surgical Sciences, Department of Surgery, Beth Israel Deaconess Medical Center, Harvard Medical School, Boston, MA 02215; [d]Institute for Human Genetics and Genomic Medicine, Medical Faculty, Rheinisch-Westfälische Technische Hochschule Aachen University, 52074 Aachen, Germany; [e]Medical Research Institute, Guangdong Provincial People's Hospital (Guangdong Academy of Medical Sciences), Southern Medical University, 510080 Guangzhou, China; [f]Institute of Pharmacology, University of Bern, 3010 Bern, Switzerland; [g]Children's and Adolescents' Hospital, University Hospital Cologne, Faculty of Medicine, University of Cologne, 50937 Cologne, Germany; [h]Cologne Center for Genomics, University of Cologne, 50931 Cologne, Germany; [i]Centre de Biotechnologie Cellulaire and CBC BioTec Biobank, Centre de Ressources Biologiques, Hospices Civils de Lyon, 69229 Lyon, France; [j]Institute of Immunology, University Hospital Heidelberg, 69120 Heidelberg, Germany; [k]Medical Department I, University Hospital Marien Hospital Herne, Ruhr-University Bochum, 44625 Herne, Germany; [l]Division of Neuropediatrics and Social Pediatrics, Department of Pediatrics, Medical Faculty, Rheinisch-Westfälische Technische Hochschule Aachen University, 52074 Aachen, Germany; [m]Department of Nephropathology, Institute of Pathology, Friedrich-Alexander Universität Erlangen-Nürnberg (FAU), 91054 Erlangen, Germany; [n]Berlin Institute of Health at Charité - Universitätsmedizin Berlin, Core Facility Genomics, 10178 Berlin, Germany; and [o]Max Delbrück Center for Molecular Medicine in the Helmholtz Association, 13125 Berlin, Germany

Author contributions: F.E., R.P.A., R.D.C., and B.B.B. designed research; F.E., R.P.A., B.R., Y.M., R.M., J.Z., C.K., M.N., L.M., A.W., S.K., N.T., G.R., I.R., J.S.-B., F.S.S., H.T., M.G.H., L.T.W., M.B.-H., M.E., S.F.C., J.A., S.H., R.D.C., and B.B.B. performed research; F.E., R.P.A., B.R., Y.M.,

R.M., J.Z., C.K., M.N., L.M., A.W., S.K., N.T., G.R., I.R., J.S.-B., F.S.S., H.T., M.G.H., L.T.W., M.B.-H., M.E., S.F.C., J.A., S.H., R.D.C., and B.B.B. analyzed data; F.E., R.P.A., R.D.C., and B.B.B. data collection; B.R., Y.M., R.M., J.Z., C.K., M.N., L.M., A.W., N.T., G.R., I.R., J.S.-B., H.T., M.B.-H., M.E., S.F.C., and J.A. data collection, manuscript editing; S.K., F.S.S., M.G.H., and L.T.W. patient care, data collection, manuscript editing; S.H. patient care, data collection; and F.E. and R.P.A. wrote the paper.

1. J. L. Johnson, Mutations in Hsp90 cochaperones result in a wide variety of human disorders. *Front. Mol. Biosci.* **8**, 787260 (2021).
2. A. Varki *et al.*, *in Essentials of Glycobiology* (Cold Spring Harbor NY, 2022).
3. A. Sudo *et al.*, Temporal requirement of dystroglycan glycosylation during brain development and rescue of severe cortical dysplasia via gene delivery in the fetal stage. *Hum. Mol. Genet.* **27**, 1174–1185 (2018).
4. N. Giovannone *et al.*, Galectin-9 suppresses B cell receptor signaling and is regulated by I-branching of N-glycans. *Nat. Commun.* **9**, 3287 (2018).
5. I. G. Ferreira *et al.*, Glycosylation as a main regulator of growth and death factor receptors signaling. *Int. J. Mol. Sci.* **19**, 580 (2018).
6. B. K. Chacko, D. W. Scott, R. T. Chandler, R. P. Patel, Endothelial surface N-glycans mediate monocyte adhesion and are targets for anti-inflammatory effects of peroxisome proliferator-activated receptor gamma ligands. *J. Biol. Chem.* **286**, 38738–38747 (2011).
7. S. E. Sparks, D. M. Krasnewich, "Congenital disorders of N-linked glycosylation and multiple pathway overview" in *GeneReviews((R))*, M. P. Adam *et al.*, Eds. (Seattle, WA, 1993).
8. T. Ju, R. D. Cummings, A unique molecular chaperone Cosmc required for activity of the mammalian core 1 beta 3-galactosyltransferase. *Proc. Natl. Acad. Sci. U.S.A.* **99**, 16613–16618 (2002).
9. Y. C. Wang *et al.*, Cosmc is an essential chaperone for correct protein O-glycosylation. *Proc. Natl. Acad. Sci. U.S.A.* **107**, 9228–9233 (2010).
10. R. P. Aryal, T. Ju, R. D. Cummings, The endoplasmic reticulum chaperone Cosmc directly promotes in vitro folding of T-synthase. *J. Biol. Chem.* **285**, 2456–2462 (2010).
11. N. Hadar *et al.*, X-linked C1GALT1C1 mutation causes atypical hemolytic uremic syndrome. *Eur. J. Hum. Genet.* (2023), 10.1038/s41431-022-01278-5.
12. U. Omasits, C. H. Ahrens, S. Muller, B. Wollscheid, Protter: Interactive protein feature visualization and integration with experimental proteomic data. *Bioinformatics* **30**, 884–886 (2014).
13. L. Xia *et al.*, Defective angiogenesis and fatal embryonic hemorrhage in mice lacking core 1-derived O-glycans. *J. Cell Biol.* **164**, 451–459 (2004).
14. W. S. Alexander *et al.*, Thrombocytopenia and kidney disease in mice with a mutation in the C1galt1 gene. *Proc. Natl. Acad. Sci. U.S.A.* **103**, 16442–16447 (2006).
15. B. R. Stotter *et al.*, Cosmc-dependent mucin-type O-linked glycosylation is essential for podocyte function. *Am. J. Physiol. Renal Physiol.* **318**, F518–F530 (2020).
16. K. Yamada *et al.*, Down-regulation of core 1 beta1,3-galactosyltransferase and Cosmc by Th2 cytokine alters O-glycosylation of IgA1. *Nephrol. Dial Transplant* **25**, 3890–3897 (2010).
17. W. Qin *et al.*, Peripheral B lymphocyte beta1,3-galactosyltransferase and chaperone expression in immunoglobulin A nephropathy. *J. Intern Med.* **258**, 467–477 (2005).
18. S. Hu *et al.*, Increased miR-374b promotes cell proliferation and the production of aberrant glycosylated IgA1 in B cells of IgA nephropathy. *FEBS Lett.* **589**, 4019–4025 (2015).
19. Y. Matsumoto *et al.*, Identification and characterization of circulating immune complexes in IgA nephropathy. *Sci. Adv.* **8**, eabm8783 (2022).
20. B. Knoppova *et al.*, The origin and activities of IgA1-containing immune complexes in IgA nephropathy. *Front. Immunol.* **7**, 117 (2016).
21. B. Knoppova *et al.*, Pathogenesis of IgA nephropathy: Current understanding and implications for development of disease-specific treatment. *J. Clin. Med.* **10**, 4501 (2021).
22. T. Ju, R. D. Cummings, Protein glycosylation: Chaperone mutation in Tn syndrome. *Nature* **437**, 1252 (2005).
23. E. G. Berger, Tn-syndrome. *Biochim. Biophys. Acta* **1455**, 255–268 (1999).
24. T. Ju, R. P. Aryal, M. R. Kudelka, Y. Wang, R. D. Cummings, The Cosmc connection to the Tn antigen in cancer. *Cancer Biomark* **14**, 63–81 (2014).
25. C. Steentoft *et al.*, Mining the O-glycoproteome using zinc-finger nuclease-glycoengineered SimpleCell lines. *Nat. Methods* **8**, 977–982 (2011).
26. T. Ju, R. P. Aryal, C. J. Stowell, R. D. Cummings, Regulation of protein O-glycosylation by the endoplasmic reticulum-localized molecular chaperone Cosmc. *J. Cell Biol.* **182**, 531–542 (2008).
27. Y. Matsumoto *et al.*, Identification of Tn antigen O-GalNAc-expressing glycoproteins in human carcinomas using novel anti-Tn recombinant antibodies. *Glycobiology* **30**, 282–300 (2020).
28. A. Novogrodsky, R. Lotan, A. Ravid, N. Sharon, Peanut Agglutinin, a new mitogen that binds to galactosyl sites exposed after neuraminidase treatment. *J. Immunol.* **115**, 1243–1248 (1975).
29. J. U. Baenziger, D. Fiete, Structural determinants of concanavalin-a specificity for oligosaccharides. *J. Biol. Chem.* **254**, 2400–2407 (1979).
30. H. Suzuki *et al.*, IgA1-secreting cell lines from patients with IgA nephropathy produce aberrantly glycosylated IgA1. *J. Clin. Invest.* **118**, 629–639 (2008).
31. J. Novak, J. Barratt, B. A. Julian, M. B. Renfrow, Aberrant Glycosylation of the IgA1 Molecule in IgA Nephropathy. *Semin Nephrol.* **38**, 461–476 (2018).
32. R. Magistroni, V. D. D'Agati, G. B. Appel, K. Kiryluk, New developments in the genetics, pathogenesis, and therapy of IgA nephropathy. *Kidney Int.* **88**, 974–989 (2015).
33. S. Lehoux *et al.*, Identification of distinct glycoforms of IgA1 in plasma from patients with immunoglobulin A (IgA) nephropathy and healthy individuals. *Mol. Cell Proteomics* **13**, 3097–3113 (2014).
34. V. Dotz *et al.*, O- and N-Glycosylation of serum immunoglobulin A is associated with IgA nephropathy and glomerular function. *J. Am. Soc. Nephrol.* **32**, 2455–2465 10.1681/ASN.2020081208 (2021).
35. K. Kiryluk *et al.*, GWAS for serum galactose-deficient IgA1 implicates critical genes of the O-glycosylation pathway. *PLoS Genet.* **13**, e1006609 (2017).
36. K. W. Wagner *et al.*, Death-receptor O-glycosylation controls tumor-cell sensitivity to the proapoptotic ligand Apo2L/TRAIL. *Nat. Med.* **13**, 1070–1077 (2007).
37. H. Trimarchi, R. Coppo, Glomerular endothelial activation, C4d deposits and microangiopathy in immunoglobulin A nephropathy. *Nephrol. Dial Transplant.* **36**, 581–586 (2021).
38. H. Suzuki *et al.*, The pathophysiology of IgA nephropathy. *J. Am. Soc. Nephrol.* **22**, 1795–1803 (2011).
39. T. Rosenblad *et al.*, Eculizumab treatment for rescue of renal function in IgA nephropathy. *Pediatr. Nephrol.* **29**, 2225–2228 (2014).
40. D. V. Rizk *et al.*, The emerging role of complement proteins as a target for therapy of IgA nephropathy. *Front. Immunol.* **10**, 504 (2019).
41. Y. L. Chiu *et al.*, Alternative complement pathway is activated and associated with galactose-deficient IgA1 antibody in IgA nephropathy patients. *Front. Immunol.* **12**, 638309 (2021).
42. S. Fuseya *et al.*, Mice lacking core 1-derived O-glycan in podocytes develop transient proteinuria, resulting in focal segmental glomerulosclerosis. *Biochem. Biophys. Res. Commun.* **523**, 1007–1013 (2020).
43. J. Zeng *et al.*, Cosmc deficiency causes spontaneous autoimmunity by breaking B cell tolerance. *Sci. Adv.* **7**, eabg9118 (2021).
44. R. Suzuki *et al.*, Global loss of core 1-derived O-glycans in mice leads to high mortality due to acute kidney failure and gastric ulcers. *Int. J. Mol. Sci.* **23**, 1273 (2022).
45. Varbank, https://varbank.ccg.uni-koeln.de/varbank2.
46. M. M. Thouin, J. M. Giron, E. P. Hoffman, Detection of nonrandom X chromosome inactivation. *Curr. Protoc. Hum. Genet.* Chapter 9, Unit 9 7 (2003).
47. C. Wehling *et al.*, Monitoring of complement activation biomarkers and eculizumab in complement-mediated renal disorders. *Clin. Exp. Immunol.* **187**, 304–315 (2017).
48. T. Ju *et al.*, A novel fluorescent assay for T-synthase activity. *Glycobiology* **21**, 352–362 (2011).